

A study of the influence of buoyancy on turbulent flow in a vertical plane passage

Jinlei Wang, Jiankang Li, J.D. Jackson *

School of Engineering, University of Manchester, Simon Building, Oxford Road, Manchester M13 9PL, UK

Abstract

A fundamental experimental study of buoyancy-aided and buoyancy-opposed turbulent flow and heat transfer to air in a vertical plane passage is reported. One wall was heated uniformly and the opposite one was unheated. Although the dominant mechanism for heat removal from the heated wall was convection, there was also some radiative heat transfer to the unheated wall. The heat received by thermal radiation was mainly removed from that wall by convection to the air flowing over it within the passage. Such a configuration has received little attention in earlier work on buoyancy-influenced flow in vertical passages. Detailed measurements of temperature were made on both walls and local values of convective heat transfer coefficient were determined on the heated surface taking careful account of the thermal radiation from it to the unheated wall and heat losses to the surroundings. A range of experimental conditions was covered over which the influence of buoyancy on the flow was systematically varied by adjusting the heat input and the mass flow rate. The mode of heat transfer ranged from forced convection with negligible influence of buoyancy to mixed convection with very strong influences of buoyancy. Profiles of velocity, turbulence intensity, turbulent shear stress and turbulence production were obtained from flow measurements made using a two-component laser Doppler Anemometer system. From these results a clear picture was arrived at of the mechanism by which the effectiveness of heat transfer was modified by the distortion of the mean flow due to the influence of buoyancy and the effect that this had on turbulence production and turbulent diffusion of heat.

© 2004 Elsevier Inc. All rights reserved.

1. Introduction

Turbulent mixed convection in vertical passages is a mode of heat transfer which is encountered in a variety of engineering applications. A good example is the cooling of nuclear reactors, where the influence of buoyancy on effectiveness of heat transfer can be a matter of considerable importance. Over the years, much attention has been concentrated on mixed convection by researchers and quite a number of studies of buoyancy-influenced heat transfer to air flowing through uniformly heated, vertical circular tubes have been reported (see, for example, Steiner, 1971; Carr et al., 1973; Easby, 1978; Jackson and Hall, 1979; Polyakov and Shindin, 1988; Jackson et al., 1989; Vil-

emas et al., 1992). As will be seen, they have yielded rather surprising results.

In the buoyancy-aided case, upward flow in a heated tube, the fluid near the surface moves faster with onset of buoyancy influence. Thus, advection (the process by which thermal energy is either accumulated or released by a moving fluid as its temperature changes), is increased. In spite of this, the effectiveness of heat transfer is reduced. This apparent anomaly can be explained by the fact that the shear stress in the layer of buoyant fluid near the surface is reduced, turbulence production is impaired and the diffusion of heat by turbulence is adversely affected (Hall and Jackson, 1969). With increase of buoyancy influence a stage is reached where the shear stress is reduced to such an extent that, having fallen to zero in the near-wall region, it becomes sufficiently negative further out for turbulence production to occur there. The effectiveness of heat transfer then improves. In the buoyancy-opposed case, downward flow in a heated tube, the motion of the fluid near the surface is retarded with the result that advection is reduced.

* Corresponding author. Tel.: +44-161-275-4307; fax: +44-161-275-4328.

E-mail address: jdjackson@man.ac.uk (J.D. Jackson).

Nomenclature

b	distance between the unheated and heated walls	T_b	bulk fluid temperature (absolute)
Bo^*	buoyancy parameter, $Gr^*/Re^{3.425}Pr^{0.8}$	u	axial component of turbulent velocity fluctuation
c_p	specific heat at constant pressure	U	axial component of time mean local velocity
C	flow and thermal development function	U_b	bulk fluid velocity
D_e	equivalent diameter, $2b$	v	transverse component of turbulent velocity fluctuation
Gr^*	Grashof number based on wall heat flux, $g\beta qD_e^4/(v^2k)$	x	axial coordinate measured from start of heating
h	heat transfer coefficient, $q/(T_w - T_b)$	y	transverse coordinate from the unheated wall
k	thermal conductivity	β	thermal expansion coefficient
Nu	Nusselt number, hD_e/k	ϵ_m	turbulent diffusivity of momentum
Pr	Prandtl number, $\mu c_p/k$	μ	absolute viscosity
P_t	turbulence production, $-\rho\bar{u}v\partial U/\partial y$	ν	kinematic viscosity, μ/ρ
Re	Reynolds number, $U_b D_e/\nu$	ρ	density
q	wall heat flux		
T_w	wall temperature (absolute)		

However, the effectiveness of heat transfer is increased. This is due to increased shear stress in the region near the surface, enhanced turbulence production and, therefore, more effective diffusion of heat by turbulence.

Some measurements of velocity and turbulence in buoyancy-aided flows have been reported which support these ideas (notably from the experiments of Carr et al. (1973) and Polyakov and Shindin (1988)). Rather surprisingly, no such measurements appear to have been reported for the buoyancy-opposed case. There is clearly a need for additional data, not only to provide more detailed confirmation of the mechanisms by which buoyancy affects turbulence and heat transfer in mixed convection but also for evaluating the advanced turbulence models and computational formulations which are now available for simulating mixed convection. The study of both buoyancy-aided and buoyancy-opposed turbulent flow and convective heat transfer reported here has yielded results which should help to satisfy this need and advance our understanding of what is an interesting and important problem. The particular configuration studied, a plane passage with one wall heated and the opposite wall adiabatic, is one where the effect of buoyancy on heat transfer could be different to that in a uniformly heated circular tube because only one boundary layer is directly affected. Also, the presence of radiant heat transfer combined with buoyancy-influenced convection adds a further interesting dimension to problem under consideration.

2. Experimental apparatus

The test section used in this investigation (see Fig. 1) was a vertical passage of rectangular cross section

612 mm by 80 mm (aspect ratio 7.65:1) and total height 4.0 m. One wall was heated over a length of 2.5 m by means of 20 separate, plate-type heaters which had an insulation pack of very low thermal conductivity material behind them to minimize heat losses to the surroundings. This was instrumented with thermocouples to enable the temperature drop across a layer of the thermal insulation material to be measured so that such losses could be accounted for. Upstream of the heated part of the test section wall was an unheated one of length 1.0 m. The opposite wall was unheated and also very well thermally insulated on the outside.

The walls were made of stainless steel sheet 3 mm thick and arranged so that they could expand freely as their temperatures changed and, therefore, remain plane. The inside surfaces of the passage had a polished mirror-like finish. The thermal emissivity of highly polished stainless steel is known to be about 0.125 in the range of temperature covered in the present study (to an accuracy of better than about 7%) from extensive measurements of the emissivity of stainless steel made earlier by the corresponding author.

Ambient air was drawn from the laboratory into the test section either at the bottom to give upward (buoyancy-aided) flow, as shown in Fig. 1, or at the top to give downward (buoyancy-opposed) flow. Downstream of the test section there was a calibrated flow-metering section (incorporating a standard, sharp edged orifice plate), a flow control valve and a blower to induce air through the test section and discharge it into the laboratory. Aluminum foil honeycomb material was installed within the unheated part of the test section at the inlet to straighten the flow.

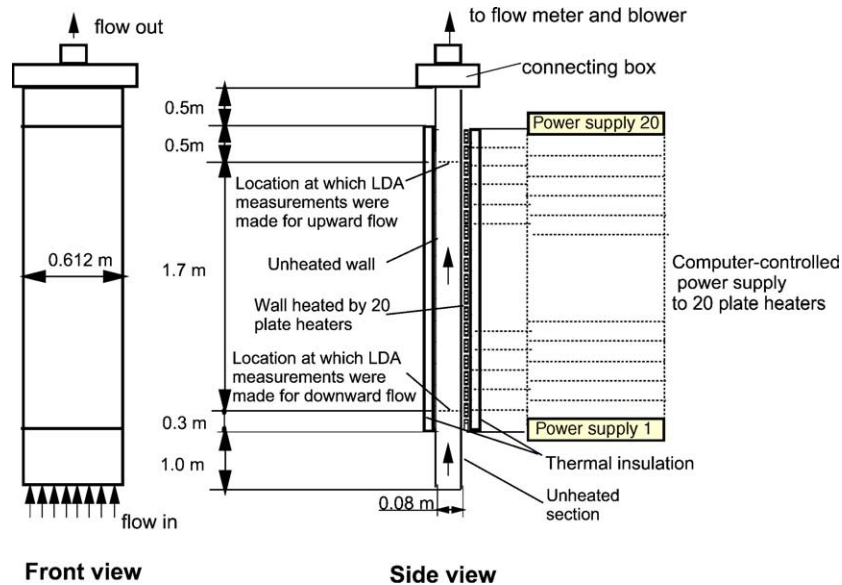


Fig. 1. Test section (upward flow arrangement).

3. Measurements

The power to each of the heaters on the test section wall could be prescribed, applied and measured by means of a multi-channel, computer-based system. In the study reported here, this was used to impose known uniform heat inputs.

Over 140 chromel–alumel thermocouples welded to the outside of the stainless steel walls of the test section enabled the temperature to be measured in detail. The value at each axial location was obtained by averaging the signals from several thermocouples to increase the accuracy. The signals from the thermocouples were supplied to a high precision data acquisition system controlled by a Pentium PC which measured the emf's to better than 5 μ V (equivalent to about one fifth of a degree).

Software was developed which combined the monitoring, data logging, power control, measurement and the data processing activities into one single package. Knowing the power input to the heated wall, its thickness and the thermal conductivity of the material, the inside surface temperature could be determined by making a correction for the temperature drop across the wall (which was quite small, the maximum value being about one third of a degree over the whole range of power input covered).

Knowing the distributions of inside surface temperature and the emissivity of the surfaces, the radiative heat transfer between the test section walls could be calculated. This was not small (up to 20% of the total power input in extreme cases). However, it could be computed quite accurately (probably to within about 5%) using the view factor approach. Of course it was necessary to assume that the surfaces were gray and

diffuse (even though they were in fact specular). As will be seen later, the heat received by the unheated adiabatic wall and mainly removed from it by convection to the air flowing within the passage did, under some conditions, lead to significant buoyancy influences on the flow near the surface.

Knowing the power input to each of the heaters (to an accuracy of better than 2%) local values of the convective heat flux from the heated wall could be determined taking account of thermal radiation and heat losses to the surroundings. The latter were also not small. They could be up to 20% of the power input under extreme conditions (with the highest heat flux at the lowest flow rate) but could be reliably accounted (to an estimated accuracy of better than about 10%) using the measured temperature differences across the instrumented layers of thermal insulation. Strictly speaking, axial conduction in the stainless steel wall also needed to be accounted for but, from the measured distributions of wall temperature, it was clear that this was a completely negligible effect. For a thermally fully developed condition with uniform heating it would be precisely zero. Thus, with the corrections described, the local convective heat flux from the heated surface could be determined to good accuracy (better than 5%).

Knowing the temperature of the ambient air drawn into the test section (to an accuracy of better than one quarter of a degree), the heat input to the air flowing through it (to an accuracy of better than about 3%) and the mass flow rate (to an accuracy of better than about 3%), local values of fluid bulk temperature could be reliably determined. Thus the wall to bulk temperature difference could be found to an estimated accuracy of better than about 3% for most of the conditions covered

(except where the flow rate was high and the heat flux was low, where the accuracy was lower, probably about 5%). Local values of convective heat transfer coefficient could therefore be determined to good accuracy (better than about 6% for most of conditions covered, decreasing to about 10% in extreme cases).

Windows were installed on one of the side walls of the test section to enable velocity and turbulence quantities to be measured using laser Doppler anemometry in the mid plane of the flow where a two-dimensional condition should be approached in a channel of aspect ratio 7.65:1. The two-component LDA system used to measure velocity consisted of a 4 W argon-ion laser generator, a transmitter, a fibre optic probe, two photomultipliers, two burst spectrum analysers and a further computer-based data acquisition system. Values of mass flow rate determined by integrating the measured profiles of velocity were found to be in good agreement with those from the orifice plate flowmeter measurements. This provided an indication that the flow was uniform from side to side across the passage.

4. Experimental programme

The LDA measurements were made point by point across the flow at a series of 33 chosen locations between the unheated and heated surfaces of the test section at an axial location about 18.5 equivalent diameters from the flow entry. From the data obtained, profiles of velocity and turbulence quantities were determined. The spacing between adjacent measurement points was varied, being much smaller near the wall than further out.

The LDA measurements commenced after the flow had been on with the seeding system operating in a stable state for some time and the laser generating system had warmed up properly. The frequency, band width, signal gain and recording length settings on the BSA units were carefully adjusted at each measuring point to enable the ratio of signal to noise to be optimized and the required validated burst rate achieved.

The LDA system was set to a mode of coincident validation of Doppler signals from the two channels. Thus, only bursts reflected from the same particle in the measuring volume were counted as validated signals. An oscillator was used to monitor the Doppler signal on line in the course of the measurements when adjusting the BSA units to try to achieve optimum performance. Enough data collection time was allowed at each measuring point to obtain reliable results (the total duration ranged from 1.5 to 2.5 h and validated burst numbers up to 50,000 were achieved). After the completion of the measurements, the data were processed using the proprietary software package available with the LDA system.

As will be seen later, the profiles of velocity and turbulence quantities obtained from the LDA mea-

surements proved to be free from significant scatter and extremely repeatable. Corresponding profiles for upward and downward flow without heating were in good agreement with each other. Profiles obtained with heating applied, under conditions where influences of buoyancy were negligible (as indicated by close agreement between corresponding profiles for upward and downward flow), proved to be in good agreement with those for unheated (isothermal) flow at the same value of Reynolds number (when compared on a normalized basis). Thus, there was plenty of evidence that the measurements obtained using the LDA system were reliable.

Some temperature profile measurements were made using a fixed rake of thermocouples at an axial location about 13 equivalent diameters from the start of heating. They were used in conjunction with the measured distributions of velocity to determine the mass weighted mean (bulk) temperature of the flow at that location. Corresponding values of bulk temperature, calculated using the steady flow energy equation knowing the net heat input to the air (the measured electrical power input minus the heat losses to the surroundings) and the mass flow rate, were found to be in satisfactory agreement with those deduced from the profiles (to within about 6%).

A comprehensive programme of experiments was completed using the test facility which yielded detailed information concerning the distributions of local heat transfer coefficient on the heated surface and profiles of velocity, turbulence and fluid temperature. A range of conditions was covered over which the influence of buoyancy on the flow varied from being negligibly small to very strong.

Measurements of velocity and turbulence were also made without any heating applied (isothermal flow). The range of Reynolds number, Re , covered was from 44,000 down to 7000 and Grashof number based on wall heat flux, Gr^* , was varied from 3.0×10^8 to 9.0×10^9 . The characteristic dimension used in defining these two dimensionless parameters was twice the spacing between the heated and unheated walls of the test section. A buoyancy parameter, Bo^* , which combined Gr^* , Re and Pr in the form $Gr^*/(Re^{3.425}Pr^{0.8})$, was used to characterise the magnitude of the buoyancy influence on the flow and heat transfer. This is based on the semi empirical model of mixed convection developed by Hall and Jackson (1969), Jackson and Hall (1979) and updated in Jackson et al. (1989). The range of Bo^* covered was from 10^{-7} to 10^{-4} .

5. Results and discussion

We begin by considering the heat transfer results. Firstly, an empirical correlation equation for developing,

variable property forced convection was established using the heat transfer data from those of the experiments performed under conditions where influences of buoyancy were negligible (ascertained by comparing profiles of velocity and turbulence quantities measured with and without heating and checking that they were closely similar). The equation obtained was

$$Nu_f = C \times 0.0228Re^{0.79}Pr^{0.4} \left(\frac{T_w}{T_b} \right)^{-0.34} \quad (1)$$

C is a function of Reynolds number and normalized axial distance from the start of heating, x/D_e . It describes the combined effect of simultaneous flow and thermal development along the test section and is given by

$$C = 1.0 + \left(\frac{x}{D_e} \right)^{-0.29} \exp \left(-0.07 \frac{x}{D_e} \right) \times \left[0.69 + \frac{5520}{Re} \left(\frac{x}{D_e} \right)^{-0.7} \right] \quad (2)$$

Next the effects of buoyancy on heat transfer were examined. This was done by plotting data in terms of Nusselt number ratio Nu/Nu_f and buoyancy parameter Bo^* . Fig. 2 provides a picture of the effects of buoyancy

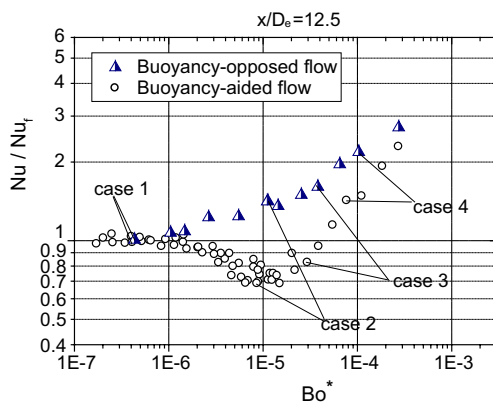


Fig. 2. Overall picture of the effects of buoyancy on heat transfer.

on heat transfer with upward and downward flow at the axial location $x/D_e = 12.5$ (where the profiles of velocity, turbulence quantities were obtained). As can be seen, impairment of heat transfer followed by recovery and enhancement of heat transfer occurred with upward flow and systematic enhancement of heat transfer oc-

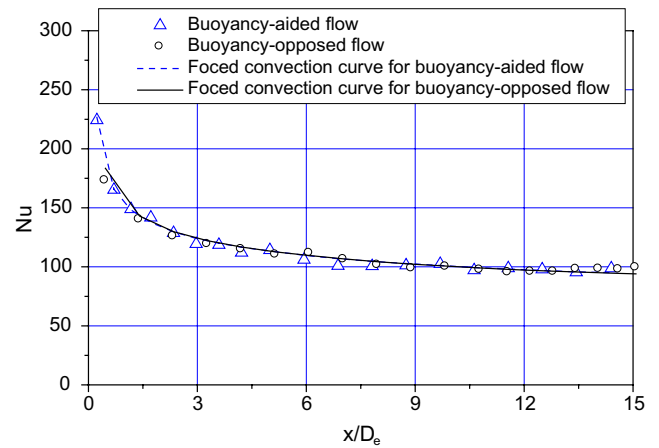


Fig. 3. Distribution of Nusselt number for Case 1.

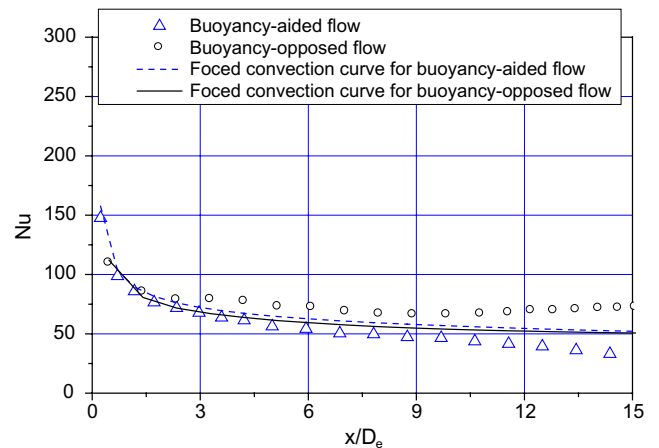


Fig. 4. Distribution of Nusselt number for Case 2.

Table 1
Experimental conditions and effects of buoyancy on heat transfer

	Flow direction	\dot{m} (kg/s)	T_{b0} (°C)	\dot{q}_{tot} (W/m ²)	Re	Gr^*	Bo^*	Nu/Nu_f
Case 1	Upward	0.238	18.1	630	43,380	2.88E+09	4.13E-07	0.99
	Downward	0.235	14.8	628	42,310	2.25E+09	4.12E-07	1.01
Case 2	Upward	0.109	20.2	1502	19,150	4.07E+09	9.72E-06	0.68
	Downward	0.111	19.8	1506	18,850	3.67E+09	1.08E-05	1.41
Case 3	Upward	0.057	18.6	449	10,160	1.50E+09	3.11E-05	0.82
	Downward	0.055	16.3	449	9770	1.30E+09	3.62E-05	1.61
Case 4	Upward	0.056	20.2	1354	9560	3.18E+09	8.06E-05	1.42
	Downward	0.053	19.3	1351	8790	2.42E+09	1.03E-04	2.18

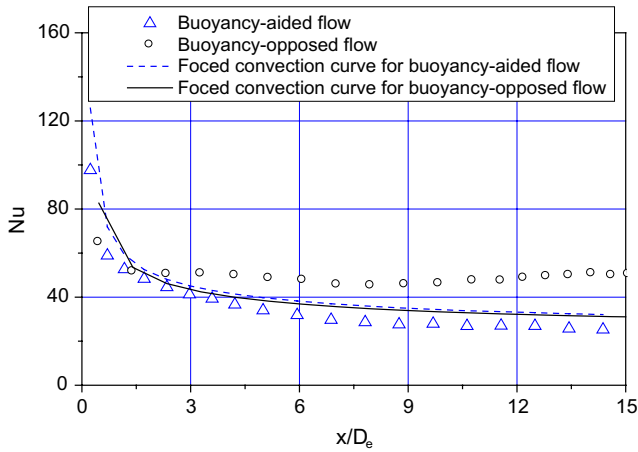


Fig. 5. Distribution of Nusselt number for Case 3.

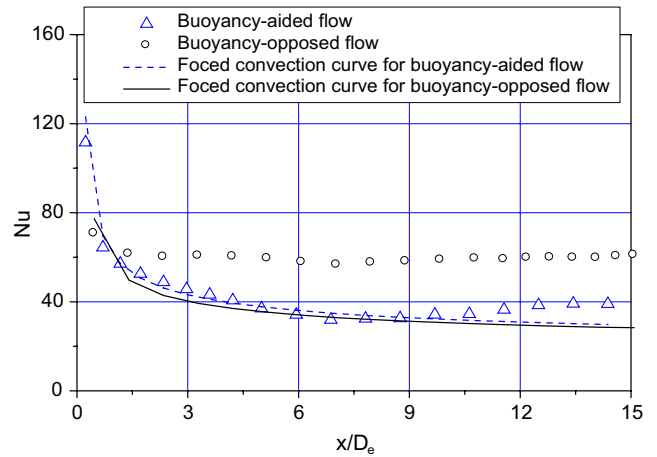


Fig. 6. Distribution of Nusselt number for Case 4.

curred with downward flow. This behaviour is similar to what has been found with heated circular tubes, but is not exactly the same. The onset of significant effects of buoyancy was delayed and occurred when Bo^* reached about 10^{-6} , as compared with a value for circular tubes of about 5×10^{-7} , and the maximum impairment of heat transfer occurred when Bo^* was about 10^{-5} , rather than about 10^{-6} .

On the basis of the picture of buoyancy-influenced heat transfer provided by Fig. 2, four particular cases were chosen from the present study for detailed consideration here. Table 1 shows the values of Re , Gr^* , Bo^* and Nu/Nu_f with upward and downward flow for each of the selected cases.

As can be seen from Fig. 2 and Table 1, there is little effect of buoyancy on heat transfer in Case 1. However,

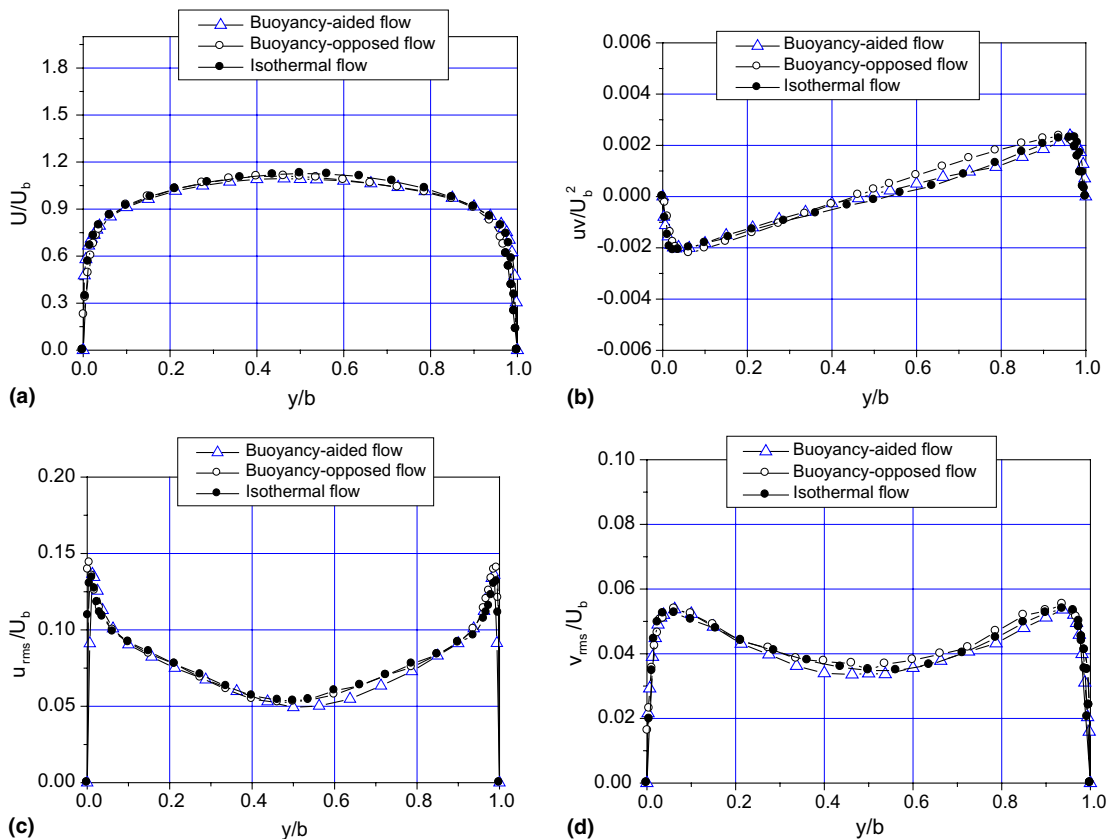


Fig. 7. Profiles of velocity and turbulence quantities for Case 1.

with increase of buoyancy influence such effects become very clearly apparent. In Cases 2 and 3, significant impairment of heat transfer is found with upward flow, being greatest in Case 2 (about 30%). There is a progressive enhancement of heat transfer with downward flow. In Case 4, heat transfer is enhanced rather than impaired with upward flow. With downward flow, it is very strongly enhanced (by a factor of over two).

Figs. 3–6 show axial distributions of Nusselt number for upward and downward flow for Cases 1 to 4, along with the corresponding distributions for forced convection (negligible influence of buoyancy) given by Eq. (1). As can be seen from Fig. 3, there is no significant difference between the results for upward and downward flow in Case 1 and the experimental data are in very good agreement with the distribution for forced convection. However, for Case 2 (Fig. 4) there is a clear difference, impairment of heat transfer developing with upward flow and enhancement with downward flow. In Case 3 (Fig. 5) the heat transfer process is again impaired with upward flow but there are signs of a recovery. With downward flow, there is further enhancement of heat transfer. In Case 4 (Fig. 6), there is clear evidence of recovery of heat transfer with upward flow, and even some enhancement in the downstream

region. With downward flow the progressive enhancement of heat transfer seen earlier continues. A fully developed thermal condition is approached in this case.

Figs. 7–10 show profiles of velocity and turbulence quantities for heated upward and downward flow along with the corresponding profiles for unheated (isothermal) flow. The heated surface is where the normalized transverse coordinate y/b has the value unity and the unheated surface is where y/b is zero.

The results for Case 1 (Fig. 7) show that the profiles of velocity and turbulence quantities with heating are the same for upward and downward flow and agree very closely with those for unheated flow. Therefore, they are not significantly affected by buoyancy.

The results for Case 2 are presented on Fig. 8. Strong distortion of the velocity profile due to buoyancy aiding the upward motion can be seen on Fig. 8(a). The modification of turbulence in buoyancy-aided flow is very clearly apparent on Fig. 8(b), which shows the profiles of normalized turbulent shear stress. In the region very close to the wall the turbulent shear stress is reduced to zero with buoyancy aiding the flow and negative stresses are present further out. Significantly increased positive stresses are present when the flow is opposed by buoyancy. The effects of buoyancy on turbulence intensity

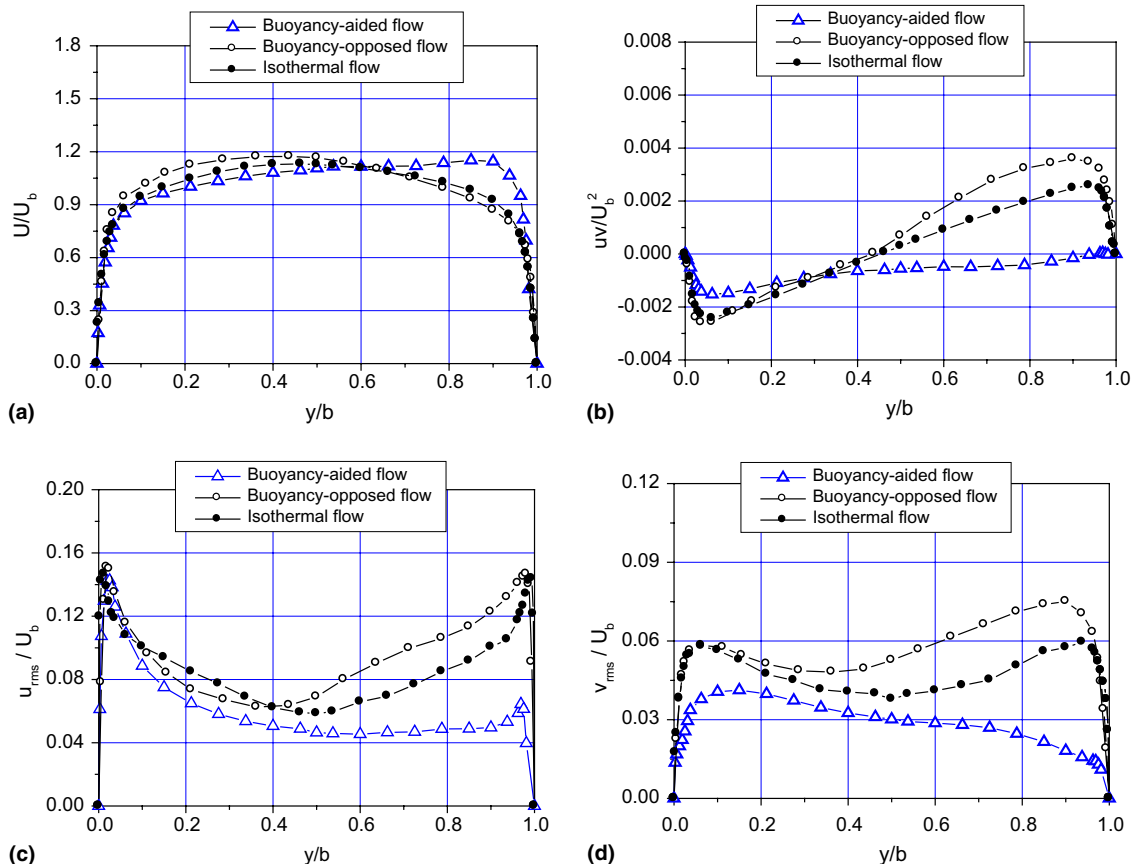


Fig. 8. Profiles of velocity and turbulence quantities for Case 2.

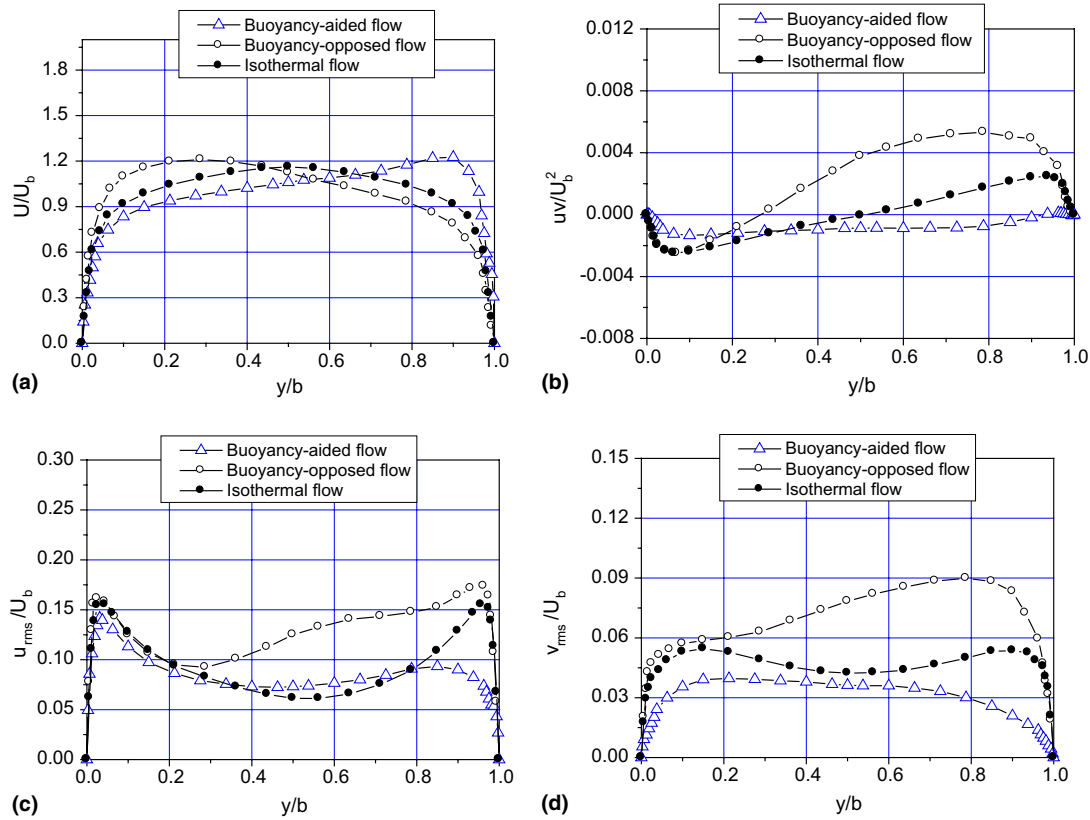


Fig. 9. Profiles of velocity and turbulence quantities for Case 3.

are very clearly apparent on Fig. 8(c) and (d), where a strong decrease can be seen with upward flow and a strong increase with downward flow, particularly in the case of the transverse component of turbulence intensity. Thus, effects of buoyancy on turbulence consistent with impairment of turbulent heat transfer with upward flow and enhancement of turbulent heat transfer with downward flow are clearly evident.

Interesting effects associated with the heat transfer by thermal radiation from the heated wall to the unheated one are apparent in the results for Case 2 (Fig. 8(b)–(d)). As mentioned earlier, the radiated heat is mainly removed from the unheated wall by the air flowing over it within the test section (the heat losses to the surroundings from that wall being very small). That this convection process is buoyancy-influenced is evident from the fact that both the turbulent shear stress and the turbulence intensities are significantly reduced on the unheated side with upward flow.

Fig. 9 shows the profiles of velocity and turbulence quantities for Case 3. The distortion of the velocity profiles due to buoyancy aiding and opposing the flow (see Fig. 9(a)) is even stronger than for Case 2, as also is the modification of the shear stress (Fig. 9(b)). With buoyancy aiding the flow, the stress is reduced to zero in the region near the heated surface and then becomes negative (but is still quite small) further out. When the

flow is opposed by buoyancy, greatly increased positive shear stresses are present. Again, influences of buoyancy on turbulence intensity are clearly apparent (Fig. 9(c) and (d)) where the effects are even stronger than for Case 2. Again effects of buoyancy reducing the turbulence on the unheated side with upward flow are evident.

Fig. 10 shows the profiles of velocity and turbulence quantities for Case 4. The distortion of the profiles due to the influence of buoyancy is even stronger. On the heated side, negative turbulent shear stresses of considerable magnitude are present when buoyancy aids the flow and, greatly increased positive turbulent shear stresses are present when buoyancy opposes it. The effects of buoyancy on turbulence intensity are equally striking. Both components of turbulence intensity are greatly increased on the heated side. Thus, effects of buoyancy on turbulence consistent with enhancement of heat transfer with both upward and downward flow are evident.

Near the unheated wall, where the incident thermal radiation is removed by convection, there is even clearer evidence of buoyancy-influenced flow. As can be seen, there is a region near the unheated wall where the turbulent shear stress is greatly reduced with upward flow and significantly increased with downward flow. Near the unheated wall very much reduced values of

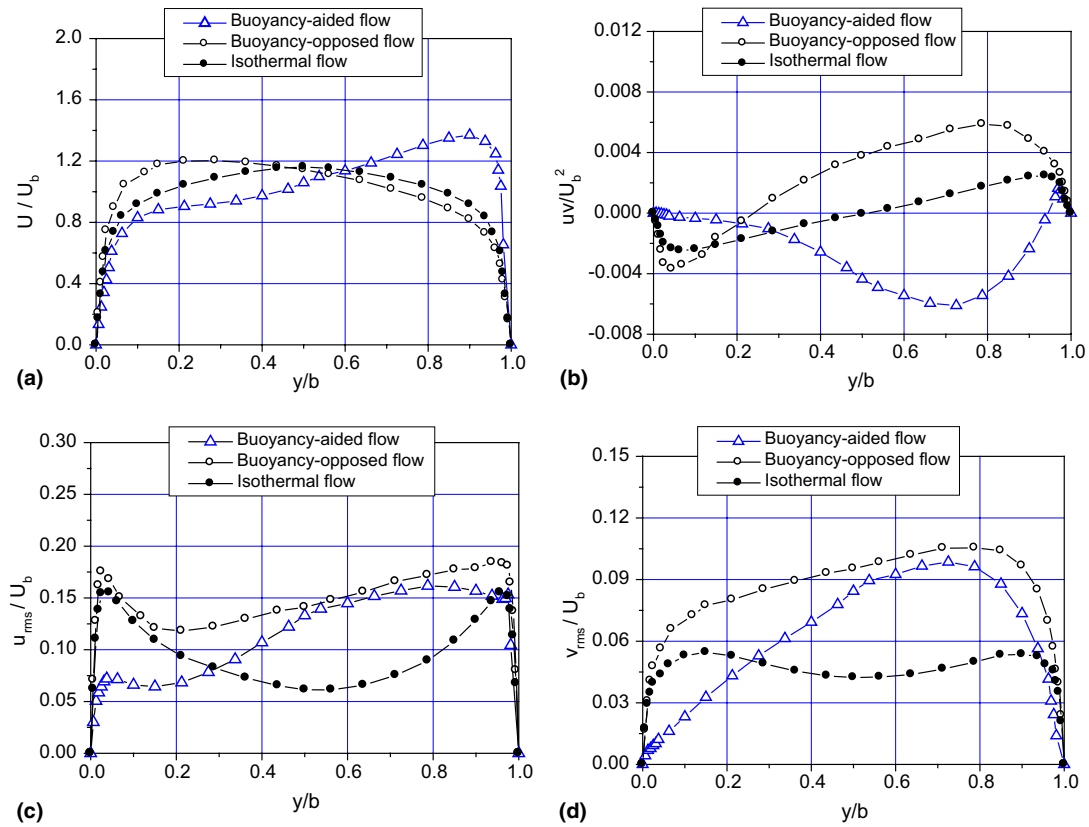


Fig. 10. Profiles of velocity and turbulence quantities for Case 4.

turbulence intensity are seen with upward flow and increased values are seen with downward flow.

That the effects of buoyancy on turbulent shear stress and turbulence intensity seen in the results presented so far are a consequence of the modification of the turbulence production can be seen by inspection of Figs. 11 and 12 which show profiles of turbulence production by the mean flow (the product of turbulent shear stress and velocity gradient) for Cases 2 and 4.

Fig. 11 shows the results for Case 2, where it can be seen that with upward flow the production of turbulence on the heated side is completely inhibited and that with downward flow it is enhanced, not only near the surface but also well away from it. In the boundary layer on the unheated wall there is evidence of reduced turbulence production with upward flow and increased turbulence production with downward flow.

Fig. 12 shows the corresponding results for Case 4, where it can be seen that, with upward flow, turbulence is produced not only in the shear layer near the heated wall but also out in the core flow well beyond the location where the velocity reaches its peak value. In both regions turbulence production with downward flow is seen to be significantly increased. Near the unheated wall, turbulence production is almost completely inhibited with upward flow but is strongly increased with

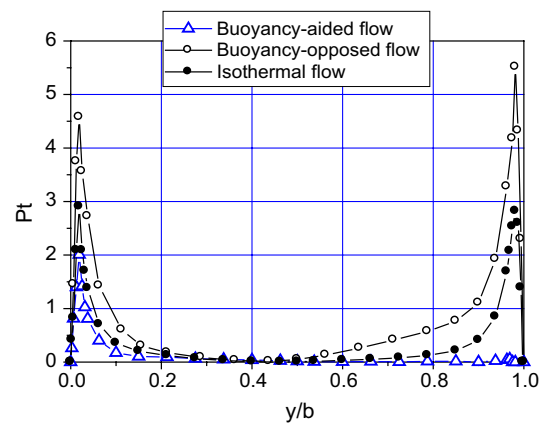


Fig. 11. Turbulence production for Case 2.

downward flow. Thus the flow in the boundary layer on the unheated wall is strongly affected by buoyancy.

The effects of buoyancy on normalized turbulent diffusivity of momentum ε_m/ν near the heated and unheated walls can be seen on Figs. 13 and 14 for Cases 2 and 4, respectively.

The results for Case 2 (Fig. 13) show that with upward flow there is a very big reduction in turbulent diffusivity near the heated surface (see Fig. 13(b)). This

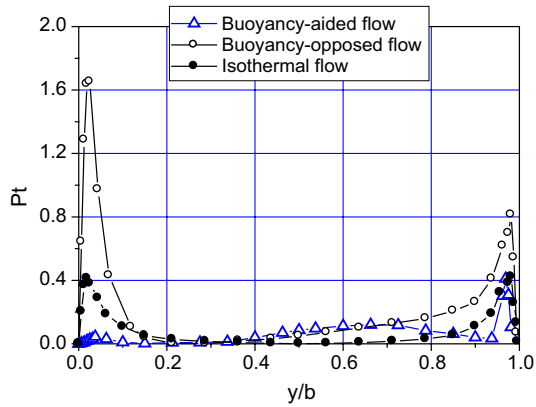


Fig. 12. Turbulence production for Case 4.

corresponds to a large increase in viscous sub-layer thickness. With downward flow there is some indication of an increase in diffusivity and therefore a decrease in sub-layer thickness, but not a large one. Near the unheated surface (Fig. 13(a)) the trends are similar but the effect is much smaller.

The results for Case 4 (Fig. 14) show that near the heated wall there is an increase of turbulent diffusivity

with both upward and downward flow (see Fig. 14(b)), whereas, near the unheated wall the turbulent diffusivity is greatly reduced with upward flow and is slightly increased with downward flow (see Fig. 14(a)).

6. Conclusions

In this study of buoyancy-influenced turbulent flow and convective heat transfer in a vertical plane passage with one wall heated and the opposite one adiabatic, it has been found that the effects on heat transfer are generally similar to those found with uniformly heated circular tubes, but are not exactly the same.

In the buoyancy-aided case (upward flow), impairment of heat transfer develops with onset of significant influence of buoyancy and this is followed by recovery of heat transfer and then enhancement of heat transfer with further increase of buoyancy influence. In the buoyancy-opposed case (downward flow) systematic enhancement of heat transfer occurs with increase of buoyancy influence. However, the effect on heat transfer is delayed in both cases compared with that for circular

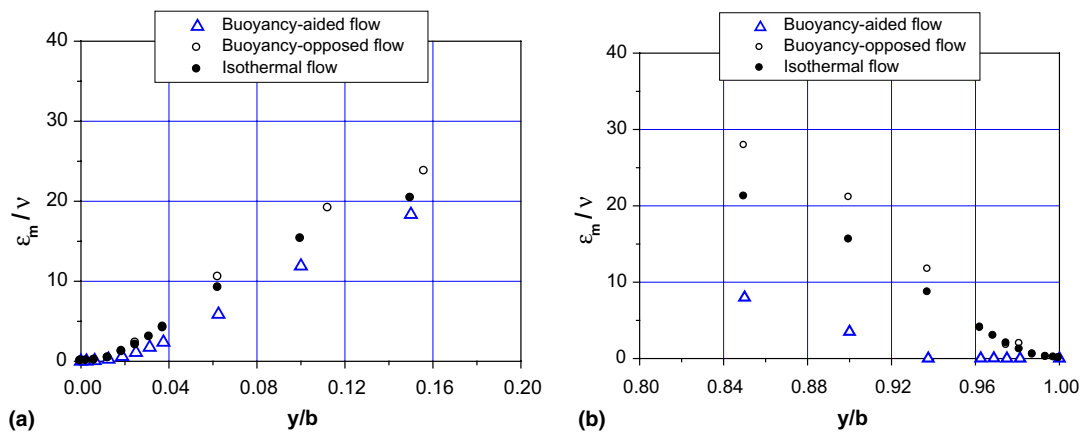


Fig. 13. Normalized turbulent diffusivity near unheated and heated surfaces for Case 2: (a) unheated surface, (b) heated surface.

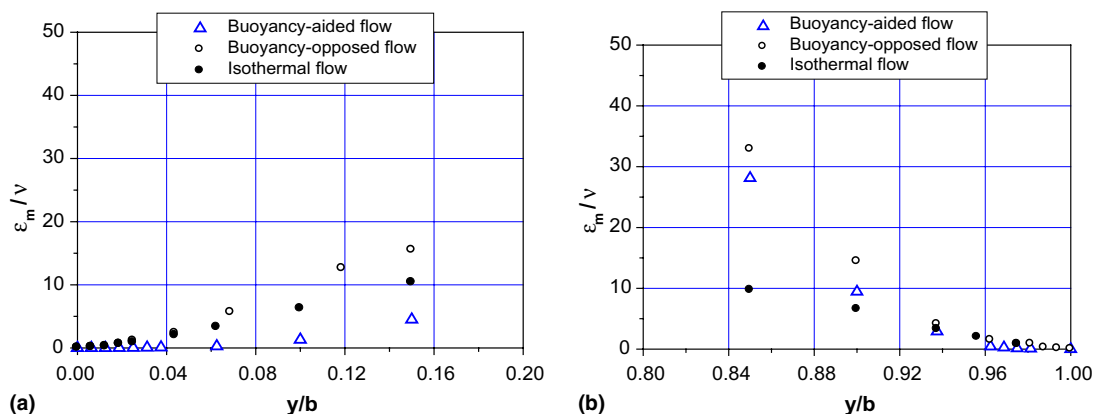


Fig. 14. Normalized turbulent diffusivity near unheated and heated surfaces for Case 4: (a) unheated surface, (b) heated surface.

tubes, probably as a result of only one boundary layer being directly affected.

Under conditions where radiative heat transfer from the heated wall to the adiabatic unheated wall becomes significant compared with the power input, the convective heat transfer process by which the radiated heat is removed from the unheated wall can, under some conditions, become buoyancy-influenced. Thus with the configuration used in the present study there is a mechanism by which interactions between radiative and convective heat transfer can occur.

The results obtained in the present study show very clearly that the dominant mechanism by which effectiveness of heat transfer is affected by buoyancy in vertical heated passages is modified turbulence production due to the distortion of the mean flow field. In the buoyancy-aided case (upward flow) this leads to either impaired or enhanced turbulent diffusion of heat, depending on the conditions. In the buoyancy-opposed case (downward flow) turbulent diffusion of heat is progressively enhanced with increase of buoyancy influence.

References

- Carr, A.D., Connor, M.A., Buhr, H.O., 1973. Velocity, temperature and turbulence measurements in air pipe flow with mixed convection. *Trans. ASME, J. Heat Transfer* 95, 445–452.
- Easby, J.P., 1978. The effect of buoyancy on heat transfer to a gas flowing down a pipe at low turbulent Reynolds numbers. *Int. J. Heat Mass Transfer* 21, 791–801.
- Hall, W.B., Jackson, J.D., 1969. Laminarization of a turbulent pipe flow by buoyancy forces. *ASME Paper*, No. 69-HT-55.
- Jackson, J.D., Hall, W.B., 1979. Influences of buoyancy on heat transfer to fluids flowing in vertical tubes under turbulent conditions. In: Kakac, S., Spalding, D.B. (Eds.), *Turbulent Forced Convection in Channels and Bundles*. Hemisphere Publishing Corp, USA, pp. 613–640.
- Jackson, J.D., Cotton, M.A., Axcell, B.P., 1989. Studies of mixed convection in vertical tubes. *Int. J. Heat Fluid Flow* 10, 2–15.
- Polyakov, A.F., Shindin, S.A., 1988. Development of heat transfer along vertical tubes in the presence of mixed air convection. *Int. J. Heat Mass Transfer* 31, 987–992.
- Steiner, A.A., 1971. On the reverse transition of turbulent flow under the action of buoyancy forces. *J. Fluid Mech.* 47, 71–75.
- Vilemas, J.V., Poskas, P.S., Kaupas, V.E., 1992. Local heat transfer in a vertical gas-cooled tube with turbulent mixed convection and different heat fluxes. *Int. J. Heat Mass Transfer* 35, 2421–2428.